

SAND2003-8146C

Symposium on Thin Films

ICM-9

9th International Conference on the Mechanical Behavior of Materials

May 25-29, 2003

Geneva Switzerland

PLASTICITY EFFECTS ON INTERFACIAL FRACTURE OF THIN GOLD FILMS

N. R. Moody, D. P. Adams*, M. J. Cordill**, D. F. Bahr**, A. A. Volinsky***

Sandia National Laboratories, Livermore, CA 94550

*Sandia National Laboratories, Albuquerque, NM 87185

**Washington State University, Pullman, WA

***Motorola, Mesa, AZ

nrmoody@sandia.gov

PLASTICITY EFFECTS ON INTERFACIAL FRACTURE OF THIN GOLD FILMS

N. R. Moody, D. P. Adams*, M. J. Cordill**, D. F. Bahr**, A. A. Volinsky***

Sandia National Laboratories, Livermore, CA 94550

*Sandia National Laboratories, Albuquerque, NM 87185

**Washington State University, Pullman, WA

***Motorola, Mesa, AZ

nrmooody@sandia.gov

ABSTRACT

A systematic study of interfacial fracture energies of thin gold films as a function of film thickness is presented in this paper. The films were sputter deposited onto sapphire substrates to thicknesses ranging from 10 nm to 200 nm. Nanoindentation was used to measure mechanical properties and combined with stressed overlayers to trigger delamination and buckling. Fracture energies and interfacial fracture energies were then obtained from the buckles using mechanics-based models. The results showed that measured fracture energies decreased with decreasing film thickness to a lower limiting value near 1.5 J/m^2 for film thicknesses up to 40 nm with a mode I normal component equal to 0.6 J/m^2 . The normal component equals the true work of adhesion and governs delamination. The shear component is composed of contributions from the test technique and crack tip plasticity which varied with film thickness.

INTRODUCTION

Gold films are the material of choice for MEMS mirrors because of their high reflectance and low residual stress levels. Nevertheless, the need to minimize stress effects requires deposition of very thin films. Most studies on gold films have focused on relatively thick films, ranging from several microns to tens of microns in thickness [1-7]. The fracture energies in these films are quite high due to extensive plasticity. However, a recent study of 200 nm thick gold films did show a marked decrease in fracture energy and posed a concern for adhesion of very thin films [8]. As a result, we have conducted a systematic study of fracture energies as a function of gold film thickness. Nanoindentation was used to measure mechanical properties and stressed overlayers were used to induce delamination and buckling. These techniques sample small volumes of material while preserving the as-deposited structures and properties of the films [9-12]. Fracture energies and interfacial toughness values were then obtained from the buckles using mechanics-based models. When combined with mechanics-based fracture models [9,10,13], the results define the relationship between structure, properties and interfacial fracture on a nanometer scale. They also help define the role of plasticity on interfacial failure of very thin ductile metal films.

MATERIALS

The gold films used in this study were sputter deposited onto smooth (0001) sapphire substrates using a d. c. magnetron sputtering unit to thicknesses ranging from 10 to 200 nm. The substrates were prepared by ultrasonic cleaning in acetone for ten minutes, in ethyl alcohol for five minutes, and then in 1M HCl for five minutes. This was followed by rinses with de-ionized water and nitrogen gas. The substrates were then annealed at 700°C in vacuum for five minutes and cooled to room temperature. This procedure reduced the number

of surface steps. The substrates were transferred to a deposition chamber and heated to 170°C in a vacuum of 1.3×10^{-5} Pa (10^{-7} torr) for two hours to drive off moisture and cooled to 30°C. This was followed by an RF backscatter for 120 s to remove contaminants and expose fresh material. With a vacuum maintained at 1.3×10^{-5} Pa (10^{-7} torr), the films were deposited at a rate of 0.3 nm/s at 1 kW using a gold target and argon as a carrier gas.

PROCEDURE

Mechanical properties were determined for each film system using the continuous stiffness measurement option on a Nano Indenter II™ with a Berkovich diamond indenter. All measurements were conducted at an excitation frequency of 45 Hz and displacement of 2 nm. Following nanoindentation testing, a tungsten overlayer was deposited on all films to provide a uniform compressive stress for fracture testing. Deposition was accomplished by placing the films in a sputter deposition chamber and heating to 170°C in vacuum to drive off moisture. Cleaning was completed with a 15 s RF backscatter to remove contaminants from the surface. The tungsten films were deposited to a thickness of 200 nm on the thickest film studied and 100 nm thick for the thinner films at a rate of 0.3 nm/s using a tungsten target and argon as the carrier gas. Deposition triggered extensive delamination and blistering in all samples. These blisters provided the data from which interfacial fracture energies were obtained using mechanics based fracture models for bilayer film systems.

RESULTS

The structure of the sputter deposited 200 nm thick gold film was previously characterized using High Resolution TEM [8]. This work showed that the films have a columnar structure and no registry across the film-substrate interface. The film-substrate interface is defined by a thin amorphous oxide layer created by the RF backscatter. AFM surface topology analysis suggests the grain size and structure are established at the earliest stages of deposition and are similar for all films of this study.

The nanoindentation results are average values from ten tests on each film. These data are given in Figure 1. The elastic modulus values show a gradual transition from film to substrate properties while the hardness values show an abrupt transition at the film substrate interface for films less than 200 nm thick. The elastic modulus and hardness values appear to converge in the near surface region and define film properties. There appears to be a small increase in modulus and hardness values with decreasing film thickness reaching a maximum in the 20 nm thick films. The small increase in values may reflect the evolution of texture and substrate properties interactions with film thickness. These values are consistent with $\langle 111 \rangle$ normal film texture [8]. The hardness values are significantly higher than observed in other studies but consistent with a 20 nm columnar grain size [8] that is less than the film thickness for all but the thinnest film tested. The small grain size also leads to the hardness values exhibiting little dependence on film thickness.

Nanoindentation was followed by sputter deposition of tungsten overlayers. The stressed overlayers constrained out-of-plane plastic flow. More importantly, they served to uniformly stress the films leading to extensive delamination and telephone cord buckling in all films tested as shown by the blisters in Figure 2 for the 10 and 200 nm thick films [14]. Optical examination on substrate fracture surfaces in all films and elemental surface analysis under the 200 nm thick blisters [8] showed that delamination occurred along the film and substrate

interface with no evidence of film-substrate interactions.

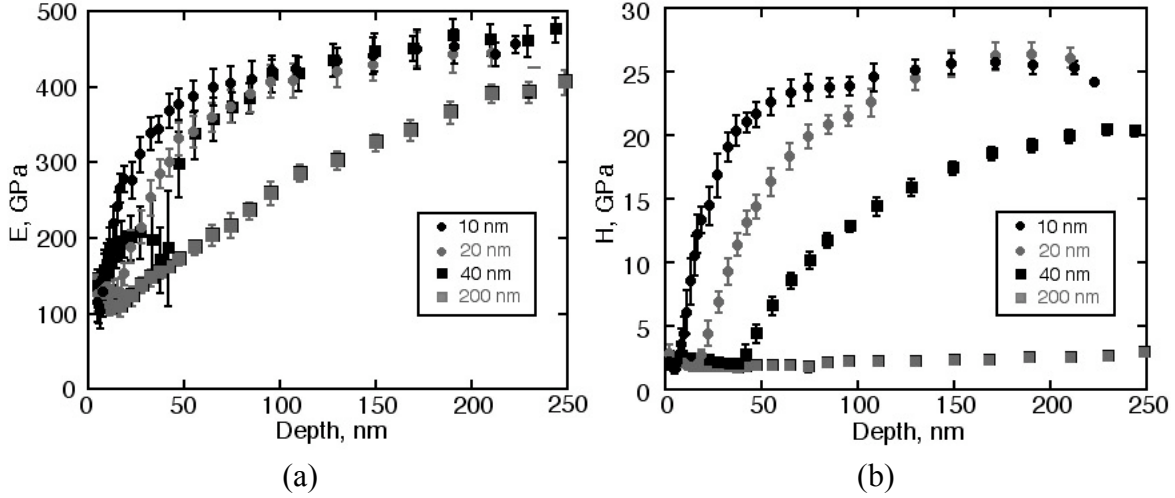


Figure 1. The (a) elastic modulus values show a gradual transition from film to substrate properties while the (b) hardness values show an abrupt transition at the film substrate interface for films less than 200 nm thick.

FRACTURE ANALYSIS

The telephone cord buckles provide the data from which interfacial fracture energies can be obtained using solutions for film systems where residual stresses dominate fracture behavior. These solutions were originally derived for single layer film-on-substrate systems [12,15,16]. Work by Bagchi et al. [11,12] and more recently by Kriese et al. [9,10] extended these solutions to multilayer systems by treating the multilayer film as a single film of the same total thickness with a transformed moment of inertia. For a blister to form between the multilayer film and substrate, the average compressive residual stress in the film system must exceed the stress for interfacial delamination [9,13] and is determined from the blister height, blister width, and film thickness [13]. Under steady state conditions, the width of the telephone cord buckle remains fixed creating a straight-sided blister with growth occurring along the more or less circular front. This gives a steady state fracture energy, γ_{ss} , as follows [13],

$$\gamma_{ss} = \frac{(1 - \nu_r^2) h \sigma_r^2}{2E} \left(\frac{\sigma_b}{\sigma_r} \right)^2 \quad (1)$$

where σ_b is the bilayer modified delamination stress, σ_r is the average residual stress in the bilayer film, h is the bilayer film thickness, and E and ν_r are the thickness weighted elastic modulus and Poisson's ratios respectively.

Using atomic force microscopy, the buckle heights and widths were measured across numerous telephone cord blisters and used to calculate the delamination and residual stresses. The residual stresses were found to be on the order of -3.4 GPa for the films in this study, consistent with residual stress levels observed in sputter deposited tungsten films of similar thickness [17].

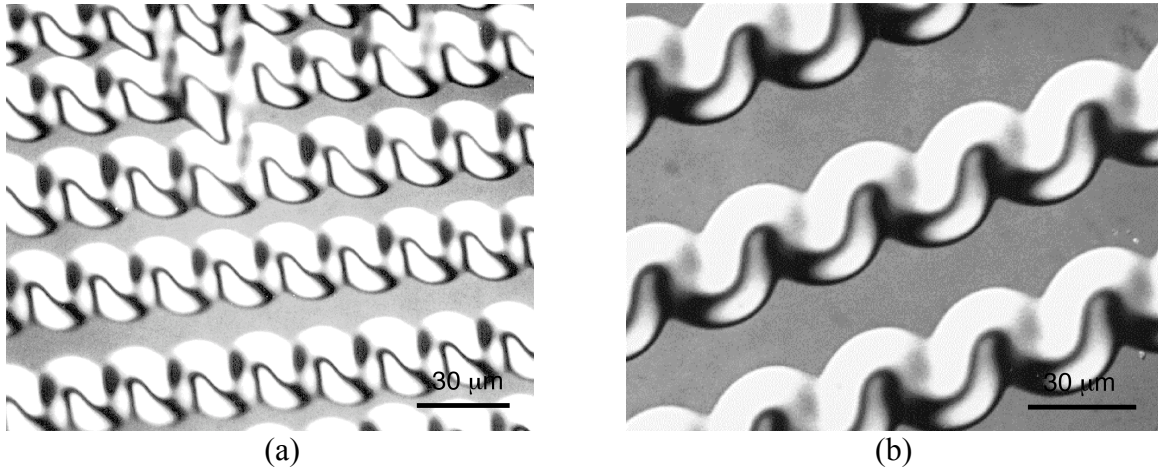


Figure 2. Telephone cord blisters triggered by sputter deposition of tungsten overlayers in (a) 10 nm and (b) 200 nm thick gold films on sapphire substrates [15].

The residual and delamination stresses were then used to calculate fracture energies. However, these are mixed mode values consisting of mode I normal and mode II shear contributions. The normal contribution is critical to understanding mechanisms controlling susceptibility to interfacial fracture. Of the criteria proposed to describe the relationship between mixed mode and normal mode I contributions, $\phi_i = \phi(\alpha) / [1 + \tan^2 \{(1 - \phi)\alpha\}]$, is most often used. In this expression, ϕ is a material parameter equal to 0.3 for most materials and α is the phase angle of loading described in previous work [13,18]. This expression was then used to calculate the mode I fracture energies. The steady state and mode I values are plotted in Figure 3 as a function of film thickness. This figure shows that the measured values exhibited a lower limiting value near 1.5 J/m^2 for film thickness up to 40 nm and increased for the 200 nm thick film. The corresponding mode I values for all films were approximately 0.5 J/m^2 . These values are within the range of true works of adhesion for gold on aluminum oxide measured in previous studies [2,3,6,19] and indicate that delamination is controlled by the true work of adhesion.

The measured stress intensities are fully capable of forming relatively large plastic zones, yet there is no evidence of ductile fracture. Suo, Shih, and Varias [20] proposed a dislocation free, elastic strip model to explain fracture in relatively thick seemingly ductile film systems where fracture appears brittle. It has recently been included with strain gradient plasticity [21] and traction-separation relationships [22,23] in a unified zone approach to interfacial fracture. The advantage of an elastic strip approach is that the crack tip is completely surrounded by elastic material and is fully characterized by local mode I normal and mode II shear stress intensity factors [24]. The near tip elasticity accommodates a large stress gradient matching nanoscopic high cohesive strength to macroscopic low yield strength [20].

Gerberich and co-workers [25] applied the concept of a dislocation free zone to explain the lower limiting plateau in fracture energies they observed in very thin copper films. With the criterion for crack tip dislocation emission developed by Rice and Thompson [26] and assuming that emitted dislocations created a dislocation free zone [27], they showed that

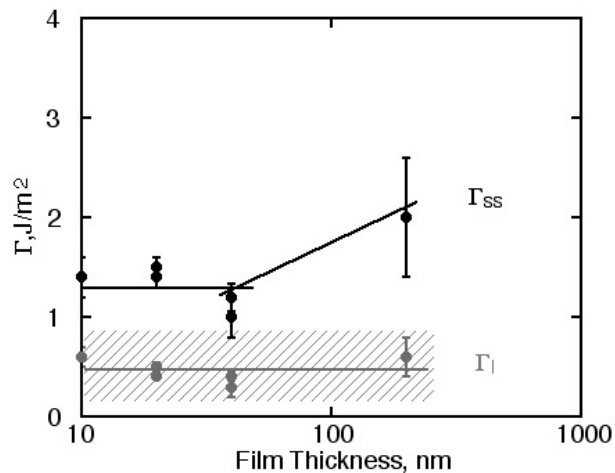


Figure 3. Steady state, Γ_{ss} , and mode I, Γ_I , fracture energies for thin gold films on sapphire. The shaded region corresponds to measured work of adhesion values.

crack tip stress intensities are not sufficient for dislocation emission in copper films up to 100 nm thick. A simple scaling of properties suggests stresses are also not sufficient for crack tip dislocation emission in gold films over the same range of film thickness. We can therefore attribute the difference between the measured mixed mode values and mode I contributions for gold films up to 40 nm thick to elastic shear contributions, necessary for stable buckle morphologies [18]. For thicker films, dislocation emission and attendant local plasticity lead to higher measured fracture energy values.

SUMMARY

We have conducted a systematic study of fracture energies as a function of gold film thickness. The films were sputter deposited onto sapphire substrates to thicknesses ranging from 10 nm to 200 nm. Nanoindentation was used to measure properties. These tests showed that elastic modulus values were near 100 GPa for all films and hardness values were near 1.8 GPa. Stressed overlayers were then sputter deposited onto the films to trigger delamination and buckling. From these buckles, fracture energies and interfacial toughness values were obtained using mechanics-based models. The results showed that measured fracture energies decreased with decreasing film thickness to a lower limiting value near 1.5 J/m² for film thicknesses up to 40 nm with a mode I normal component equal to 0.6 J/m² for all film thickness tests. Comparison with previous work, shows that the lower limiting plateau in fracture energies results from conditions which preclude crack tip dislocation emission. The normal component equals the true work of adhesion and governs delamination. To this are added elastic shear contributions from stable buckle formation and contributions from crack tip plasticity, which vary with film thickness.

ACKNOWLEDGEMENT

The authors thank Prof. W. W. Gerberich from the University of Minnesota for helpful discussions. The authors also gratefully acknowledge the support from the U.S. Department of Energy through Contract DE-AC04-94AL85000.

REFERENCES

- [1] H. M. Jensen, J.W. Hutchinson, and K.-S. Kim, *Int. J. Solids Struct.*, vol 26, pp. 1099-1114, 1990.
- [2] I. E. Reimanis, B. J. Dalgleish, M. Brahy, M. Ruhle, and A. G. Evans, *Acta Metall. Mater.*, vol 38, pp. 2645-2652, 1990.
- [3] I. E. Reimanis, B. J. Dalgleish, and A. G. Evans, *Acta Metall. Mater.*, vol 39, pp. 3133-3141, 1991.
- [4] A. G. Evans and B. J. Dalgleish, *Acta Metall. Mater.*, vol 40, pp. S295-S306, 1992.
- [5] S. X. Mao and A. G. Evans, *Acta Mater.*, vol 45, pp. 4263-4270, 1997.
- [6] D. M. Lipkin, D. R. Clarke, and A. G. Evans, *Acta Mater.*, vol 46, pp. 4835-4850, 1998.
- [7] M. R. Turner and A. G. Evans, *Acta Mater.*, vol 44, pp. 863-871, 1996.
- [8] N. R. Moody, D. P. Adams, D. Medlin, A. A. Volinsky, N. Yang, and W. W. Gerberich, *Int. J. Fract.*, 2003, to be published.
- [9] M. D. Kriese, W. W. Gerberich, and N. R. Moody, *J. Mater. Res.*, vol 14, pp. 3007-3018, 1999.
- [10] M. D. Kriese, N. R. Moody, and W. W. Gerberich, *Acta Mater.*, vol 46, pp. 6623-6630, 1998.
- [11] A. Bagchi and A. G. Evans, *Thin Solid Films*, vol 286, pp. 203-212, 1996.
- [12] A. Bagchi, G. E. Lucas, Z. Suo, and A. G. Evans, *J. Mater. Res.*, vol 9, pp. 1734-1741, 1994.
- [13] J. W. Hutchinson, Z. Suo, in *Advances in Applied Mechanics*, J. W. Hutchinson and T. Y. Wu, eds., Academic Press Inc., New York, vol 29, pp. 63-191, 1992.
- [14] A. A. Volinsky, D. F. Bahr, M. D. Kriese, N. R. Moody, W. W. Gerberich, in *Encyclopedia of Comprehensive Structural Integrity*, I. Milne and R. O. Ritchie, and B. Karihaloo, eds. vol 8, ch 13, Elsevier, to be published.
- [15] D. B. Marshall and A. G. Evans, *J. Appl. Phys.*, vol 56, pp. 2632-2638, 1984.
- [16] A. G. Evans and J. W. Hutchinson, *Int. J. Solids Struct.*, vol 20, pp. 455-466, 1984.
- [17] R. C. Sun, T. C. Tisone, and P. D. Cruzan, *J. Appl. Phys.*, vol 46, pp. 112-117, 1975.
- [18] M. D. Thouless, J. W. Hutchinson, and E. G. Liniger, *Acta Metall. Mater.* vol 40, pp. 2639-2649, 1992.
- [19] R. M. Pilliar and J. Nutting, *Phil Mag.*, vol 16, pp. 181-188, 1967.
- [20] Z. Suo, C. V. Shih, and A. G. Varias, *Acta Metall. Mater.*, vol 41, pp. 1551-1557, 1993.
- [21] Y. Wei and J. W. Hutchinson, *J. Mech. Phys. Solids*, vol 45, pp. 1137-1159, 1997.
- [22] Y. Wei and J. W. Hutchinson, *Int. J. Fracture.*, vol 95, pp. 1-17, 1999.
- [23] A. G. Evans, J. W. Hutchinson, and Y. Wei, *Acta Mater.*, vol 47, pp. 4093-4113, 1999.
- [24] M. Y. He, A. G. Evans, and J. W. Hutchinson, *Acta Mater.*, vol 44, pp. 2963-2971, 1996.
- [25] W. W. Gerberich, A. A. Volinsky, N. I. Tymiak, and N. R. Moody, in *Thin Films- Stresses and Mechanical Properties VIII*, R. Vinci, O. Kraft, N. Moody, P. Besser, and E. Schaffer II, eds., Materials Research Society, Pittsburgh, PA, vol 594, pp. 351-364, 2000.
- [26] J. R. Rice and R. Thompson, *Phil. Mag.*, vol 29, pp. 73-97, 1974.
- [27] A. A. Volinsky, N. R. Moody, and W. W. Gerberich, *Acta Mater.*, vol 50, pp. 441-466, 2002.